Accurate, Robust, and Reliable Calculations of Poisson–Boltzmann Binding Energies

Duc D. Nguyen,[a]† Bao Wang,[a]† and Guo-Wei Wei ⓘ*[a,b,c]

Poisson–Boltzmann (PB) model is one of the most popular implicit solvent models in biophysical modeling and computation. The ability of providing accurate and reliable PB estimation of electrostatic solvation free energy, ΔG_{el}, and binding free energy, $\Delta\Delta G_{el}$, is important to computational biophysics and biochemistry. In this work, we investigate the grid dependence of our PB solver (MIBPB) with solvent excluded surfaces for estimating both electrostatic solvation free energies and electrostatic binding free energies. It is found that the relative absolute error of ΔG_{el} obtained at the grid spacing of 1.0 Å compared to ΔG_{el} at 0.2 Å averaged over 153 molecules is less than 0.2%. Our results indicate that the use of grid spacing 0.6 Å ensures accuracy and reliability in $\Delta\Delta G_{el}$ calculation. In fact, the grid spacing of 1.1 Å appears to deliver adequate accuracy for high throughput screening. © 2017 Wiley Periodicals, Inc.

Introduction

Electrostatics is ubiquitous in biomolecular and cellular systems and of paramount importance to biological processes. Accurate and reliable prediction of electrostatic binding free energy, $\Delta\Delta G_{el}$, is crucial to biophysical modeling and computation. The prediction of $\Delta\Delta G_{el}$ plays a vital role in the study of many cellular processes, such as signal transduction, gene expression, and protein synthesis. Additionally, many pharmaceutical applications, especially in the final stage of the drug design, rely on the accurate and reliable calculation of binding free energy. Technically, the accuracy and reliability of electrostatic binding energy prediction depend essentially on the quality of electrostatic solvation (ΔG_{el}) estimation, which can be achieved by solving the Poisson–Boltzmann (PB) equation in the implicit solvent model.[1–5] In past decades, the development of a robust PB solver catches much attention in computational biophysics and biochemistry. Mathematically, most PB solvers reported in the literature are based on three major approaches, namely, the finite difference method (FDM),[6] the finite element method,[7,8] and the boundary element method (BEM).[9,10] Among them, the FDM is prevalently used in the field due to its simplicity in implementation. The emblematic solvers in this category are Amber PBSA,[11,12] Delphi,[13,14] APBS,[15] and CHARMM PBEQ.[6]

In the past few years, there have been many attempts to develop highly accurate PB solvers using advance techniques for interface treatments.[16,17] However, no confirmation for the reliable use of grid spacing of 0.5 Å in $\Delta\Delta G_{el}$ has been given. In this work, we investigate the grid dependence of our PB solver (MIBPB)[4,18] in estimating both electrostatic solvation free energies and electrostatic binding free energies. The MIBPB solver is by far the only existing method that is second-order accurate in L_∞ norm for solving the PB equation with discontinuous dielectric constants, singular charge sources, and geometric singularities from the solvent excluded surfaces (SESs) of biomolecules.[18] Here, the L_∞ norm means the maximum absolute error measure and "second order accurate" means that the error reduces four times when the grid spacing is halved. Our results indicate that the use of grid spacing 0.6 Å ensures accuracy and reliability in $\Delta\Delta G_{el}$ calculation. In fact, a grid spacing of 1.1 Å appears to deliver adequate accuracy for high throughput screening. We, therefore, believe that when it is used properly, the PB methodology is able to deliver accurate and reliable electrostatic binding analysis.

Theory and Methods

The PB model

The PB model is a multiscale model. In this model, the solvent is treated as a dielectric continuum while the solute molecule is described at the atomistic detail.[1,4] Denote Ω_m and Ω_s, respectively, as the solute and solvent domains. The computational domain $\Omega \in \mathbb{R}^3$ is, then, formed by $\Omega = \Omega_m \cup \Gamma \cup \Omega_s$, where Γ is the molecular surface. If the ion-exclusive layer is ignored, one can formulate the PB equation as follows

[a] D. D. Nguyen, B. Wang, G.-W. Wei
    Department of Mathematics, Michigan State University, Michigan 48824
    E-mail: wei@math.msu.edu
[b] Guo-Wei Wei
    Department of Electrical and Computer Engineering, Michigan State University, Michigan 48824
[c] Guo-Wei Wei
    Department of Biochemistry and Molecular Biology, Michigan State University, Michigan 48824

†These authors contributed equally to this work.

$$-\nabla \cdot (\varepsilon(\mathbf{r})\nabla\phi(\mathbf{r})) + \kappa^2(\mathbf{r})\left(\frac{k_B T}{e_c}\right)\sinh\left(\frac{e_c\phi(\mathbf{r})}{k_B T}\right) = 4\pi\sum_{i=1}^{N_m} q_i \delta(\mathbf{r}-\mathbf{r}_i),$$
(1)

where $\phi(\mathbf{r})$ is the electrostatic potential and q_i is the partial charge of the ith atom at position $\mathbf{r}_i$. In addition, constants $k_B, T, e_c,$ and N_m are, respectively, the Boltzmann constant, the absolute temperature, the electronic charge, and the number of charges in the biomolecule. The dielectric coefficient $\varepsilon(\mathbf{r})$ and the ionic strength $\kappa(\mathbf{r})$ are defined as

$$\varepsilon(\mathbf{r}) = \begin{cases} \varepsilon_m, & \mathbf{r} \in \Omega_m; \\ \varepsilon_s, & \mathbf{r} \in \Omega_s, \end{cases}$$
(2)

and

$$\kappa(\mathbf{r}) = \begin{cases} 0, & \mathbf{r} \in \Omega_m; \\ \bar{\kappa}, & \mathbf{r} \in \Omega_s, \end{cases}$$
(3)

where $\bar{\kappa}$ is the Debye–Huckel parameter.

The far-filed boundary condition $\phi(\infty)=0$ is used for PB eq. (1). However, for a practical computation, the following Debye–Huckel boundary condition is carried out

$$\phi(\mathbf{r}) = \sum_{i=1}^{N_m} \frac{q_i}{\varepsilon_s |\mathbf{r}-\mathbf{r}_i|} e^{-\bar{\kappa}|\mathbf{r}-\mathbf{r}_i|}$$
(4)

Moreover, the interface conditions across the solvent-solute interface Γ are imposed as

$$[\phi(\mathbf{r})] = 0, \quad \mathbf{r} \in \Gamma;$$
(5)

$$[\varepsilon(\mathbf{r})\nabla\phi(\mathbf{r})] \cdot \mathbf{n} = 0, \quad \mathbf{r} \in \Gamma,$$
(6)

where $[\ast]$ denotes the difference of the quantity $\ast$ cross the interface, and $\mathbf{n}$ is the normal vector pointing out from solute region to solvent region.

The electrostatic solvation free energy in the PB model can be expressed as

$$\Delta G_{el} = \frac{1}{2}\sum_{i=1}^{N_m} q_i(\Phi(\mathbf{r_i}) - \Phi_0(\mathbf{r_i})),$$
(7)

where Φ_0 is the solution of the PB equation without considering the solvent-solute interface.

MIBPB package

In the current work, we use the our MIBPB package[4,18] to predict the electrostatic solvation free energy. The MIBPB package is a second-order convergence PB solver for dealing with the SESs of biomolecules. Numerically, there are three major obstacles in constructing accurate and reliable PB solvers. First, commonly used solvent-solute interfaces, that is, the van der Walls surface, solvent accessible surface, and the SES[19,20] admit geometric singularities, such as sharp tips, cusps and self-intersecting surfaces,[21] which make the rigorous

enforcement of interface jump conditions a formidable task in PB solvers. An advanced mathematical interface techniques, the matched interface and boundary (MIB) method,[22–27] is used in the MIBPB package to achieve the second order accuracy in handling biomolecular SESs. Specifically, the MIB method uses the Cartesian grid for the finite difference (FD) schemes. However, in the vicinity of the interface, the regular FD algorithm will fail to achieve its designed accuracy. To overcome this hindrance, the jump conditions (5) and (6) are rigorously enforced in the MIB algorithm to restore the designed order of convergence. To this end, we classify the grid points (or nodes) into two categories, regular ones and irregular ones. A node is irregular when its FD expression involves node(s) on the other side of the interface. The MIB method replaces the value of an irregular point by a linear combination of regular ones and jump conditions, and refers it as a fictitious value. As a result, the designed accuracy can be restored under that treatment.[22–27] Additionally, the atomic singular charges described by the Dirac delta functions give rise to another difficulty in constructing highly accurate PB solver. A Dirichlet-to-Neumann map technique has been developed in the MIBPB package to avoid the direct numerical approximation of singular charges using the analytical Green's functions.[28] Finally, the nonlinear Boltzmann term can affect solver efficiency when handled inappropriately, particularly for BEMs. A quasi-Newton algorithm is implemented in the MIBPB package[4,18] to take care the nonlinear term.[4,18] The second order convergence in L_∞ norm of the MIBPB solver for the electrostatic potential and electrostatic solvation free energy of realistic protein SESs was confirmed in our earlier work.[26,28] Interested readers can access this package via our online server at http://weilab.math.msu.edu/MIBPB/.

Interface generation

Many studies suggest that SES is able to deliver the state of the art accurate modeling of the solvated molecule.[7,10,14] As a result, much effort has been paid to developing an accurate and robust SES software.[21,29] However, the MSMS software[21] generates a Lagrangian representation of the SES and is inconvenient for the Cartesian domain implementation of PB solvers. A Lagrangian to Eulerian transformation is required to convert MSMS surfaces for our Cartesian-based MIBPB solver.[4] Most recently, we have developed a new SES software, Eulerian solvent excluded surface (ESES), to directly generate the SESs in the Eulerian representation.[30] Our ESES software enables the MIBPB solver to produce a reliable ΔG_{el}. Both MSMS and ESES are supported by our MIBPB software. By increasing the MSMS surface density, the electrostatic solvation free energies calculated using MSMS converge to those obtained using ESES.[30] Therefore, only results using ESES are shown in this work. Our ESES online server is available at http://weilab.math.msu.edu/ESES/.

Datasets

In the present work, we use three sets of biomolecular complexes for solvation free energy and binding free energy
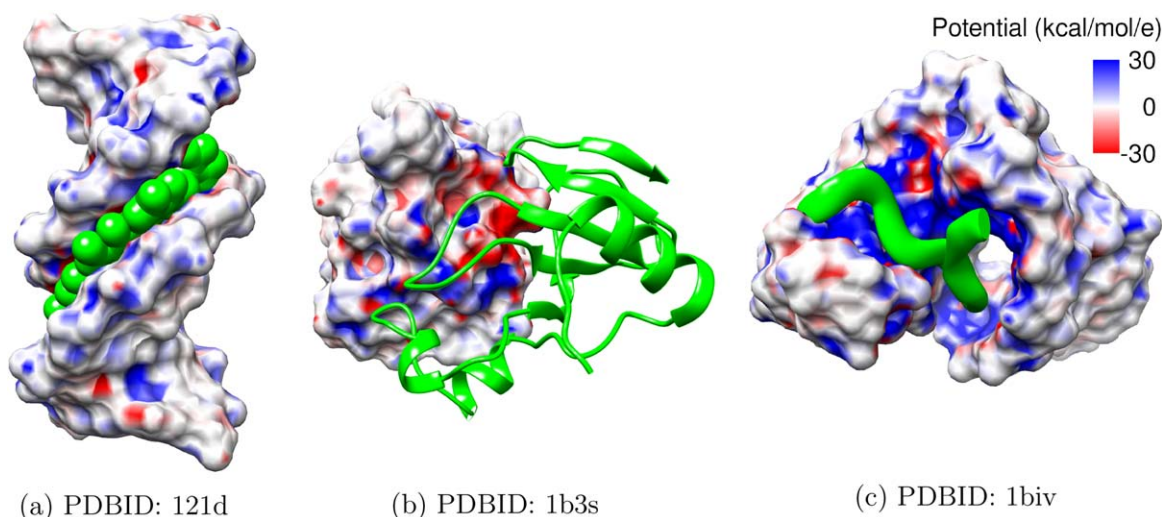
Figure 1. Illustration of surface electrostatic potentials (in units of kcal/mol/e) for three complexes, generated by Chimera software.[31] a) PDBID: 121d (in Drug-DNA complexes); b) PDBID: 1b3s (in barnase-barstar complexes); c) PDBID: 1biv (in RNA-peptide complexes). [Color figure can be viewed at wileyonlinelibrary.com]

estimations. Specifically, the first set, Dataset 1, is a collection of DNA-minor groove drug complexes having a narrow range of $\Delta\Delta G$. The Protein Data Bank (PDB) IDs (PDBIDs) for this set are as follows: 102d, 109d, 121d, 127d, 129d, 166d, 195d, 1d30, 1d63, 1d64, 1d86, 1dne, 1eel, 1fmq, 1fms, 1jtl, 1lex, 1prp, 227d, 261d, 164d, 289d, 298d, 2dbe, 302d, 311d, 328d, and 360d. The second set, Dataset 2, includes various wild-type and mutant barnase-barstar complexes. Its PDBIDs are as follows: 1b27, 1b2s, 1b2u, 1b3s, 2az4, 1x1w, 1x1y, 1x1u, and 1x1x. In the last set, Dataset 3, we investigate RNA-peptide complexes with following PDBIDs: 1a1t, 1a4t, 1biv, 1exy, 1g70, 1hji, 1i9f, 1mnb, 1nyb, 1qfq, 1ull, 1zbn, 2a9x, and 484d. The datasets can be downloaded from website http://www.sb.fsu.edu/m~fenley/convergence/downloads/convergence_pqr_sets.tar.gz. They are also available from our website http://users.math.msu.edu/users/wei/Data/bindingdata.tar.gz.

PB calculation details

The electrostatics binding free energy is a measure of binding affinity of two compounds due to the electrostatics interaction. Based on the free energy cycle, the electrostatics binding free energy can be calculated by the following formula

$$\Delta\Delta G_{el} = (\Delta G_{el})_{AB} - (\Delta G_{el})_A - (\Delta G_{el})_B + (\Delta\Delta G_{el})_{Coulomb}, \quad (8)$$

where $(\Delta G_{el})_{AB}$ is the electrostatic solvation free energy of the bounded complex AB, $(\Delta G_{el})_A$ and $(\Delta G_{el})_B$ are the electrostatic solvation free energies of the unbounded components A and B, and $(\Delta\Delta G_{el})_{Coulomb}$ is the electrostatic binding free energy of the two components in vacuum.

The electrostatic solvation free energies ΔG_{el} are obtained using MIBPB software[4,18] while the binding energy $(\Delta\Delta G_{el})_{Coulomb}$ is easily evaluated analytically via the following formula

$$(\Delta\Delta G_{el})_{Coulomb} = \sum_{i,j} \frac{q_i q_j}{\varepsilon_m r_{ij}}, \quad \forall i \in A, j \in B, \quad (9)$$

where q_i and q_j are the corresponding charges of the given pair of atoms, and r_{ij} is the distance between this pair. Here, ε_m is the dielectric constant of the solute region. Table S3 (in the Supporting Information) lists $(\Delta\Delta G_{el})_{Coulomb}$ values of 51 studied complexes.

In all our calculations, the absolute temperature of the ionic solvent is chosen to be $T = 298$ K, the dielectric constants for solute and solvent are 1 and 80, and the ionic strength is 0.1 M NaCl. The PBE is solved by the linearized solver, but the nonlinear one does not produce any notably differences. The incomplete LU biconjugate gradient squared (ILUBGS) solver is used to solve all linear systems risen by the MIBPB approach. To maintain consistent computations of the PB solver at different grid sizes, the criteria convergence of ILUBGS solver measured by L_2-norm is set to be 10^{-6}, and the maximum iteration number is set to 100,000. The predictions of MIBPB solver on ΔG_{el} and $\Delta\Delta G_{el}$ are confirmed by other solvers such as PBSA,[11,12] Delphi,[13,14] and APBS[15] at the grid size of 0.2 Å, see Table S2 of Supporting Information.

Results and Discussion

As described above, we consider three sets of binding complexes, namely, drug-DNA, barnase-barstar and RNA-peptide systems. For the sake of illustration, three sample surface electrostatic potentials, each from one distinct set, are depicted in Figure 1. PDBIDs for these three complexes are respectively 121d (in Drug-DNA complexes), 1b3s (in barnase-barstar complexes), and 1biv (in RNA-peptide complexes). In the rest of this section, we explore the influence of grid spacing in PB equation solvation and binding free energy estimations using our MIBPB solver.
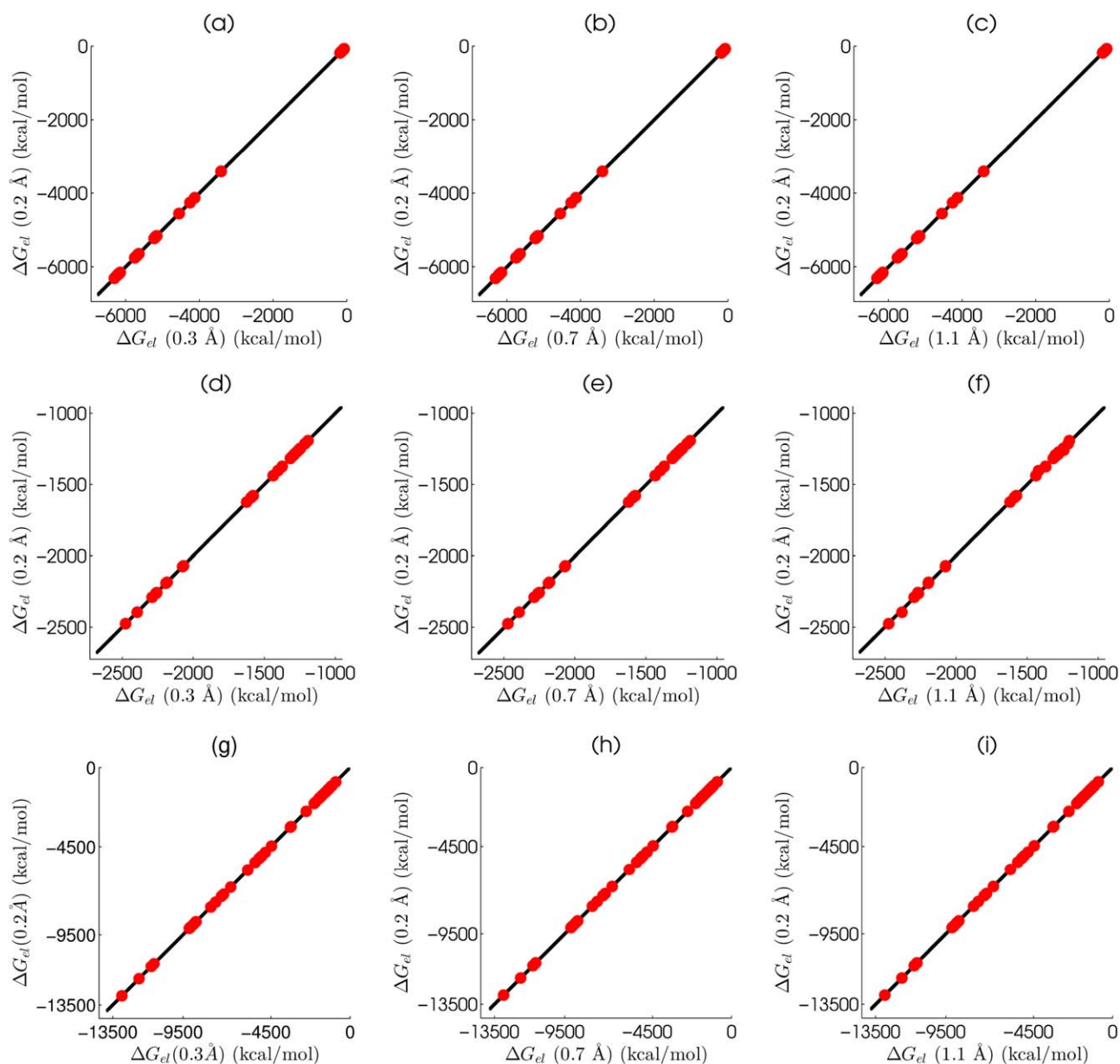
Figure 2. Electrostatic solvation free energy, for all complexes and unbounded components of three datasets, with different grid sizes plotted against the one computed with a finest grid size of $h=0.2$ Å. a) DNA-drug with pair (0.2 Å, 0.3 Å); b) DNA-drug with pair (0.2 Å, 0.7 Å); c) DNA-drug with pair (0.2 Å, 1.1 Å); d) Barnase-barstar with pair (0.2 Å, 0.3 Å); e) Barnase-barstar with pair (0.2 Å, 0.7 Å); f) Barnase-Barstar with pair (0.2 Å, 1.1 Å); g) RNA-peptide with pair (0.2 Å, 0.3 Å); h) RNA-peptide with pair (0.2 Å, 0.7 Å); i) RNA-peptide with pair (0.2 Å, 1.1 Å). [Color figure can be viewed at wileyonlinelibrary.com]

The influence of grid spacing in ΔG_{el} estimation

We first examine the accuracy and robustness of our MIBPB solver in predicting the electrostatic solvation free energies of the aforementioned three datasets. Some previous literature[32,33] has recognized that a grid size of $h=0.5$ Å is small enough to produce a reliable ΔG_{el}. Such an observation certainly remains for the MIBPB solver. In fact, our PB solver is able to deliver a very well-convergent calculations of electrostatic solvation free energies at as coarse grid sizes as 1.0 and 1.1 Å.

In the current calculations, the finest grid size is chosen to be 0.2 Å, and the coarser grid sizes are between 0.3 and 1.1 Å. Figure 2 depicts the correlations of ΔG_{el} at various meshes for

all complexes and unbounded components of three datasets. The electrostatic solvation free energies obtained at the finest grid spacing of 0.2 Å are plotted against those computed from coarser grid spacings of 0.3, 0.7, and 1.1 Å. Obviously, the best fitting lines for these data at various coarse grid spacings produce nearly perfect alignments between the finest mesh results and those from coarse meshes. As shown in Table 1, R^2 and slope values at the pair of grid sizes (0.2 Å, 1.1 Å) for DNA-drug, barnase-barstar and RNA-peptide are, respectively, $(1.0000, 1.0004)$, $(0.9997, 0.9972)$, and $(1.0000, 1.0005)$. These results indicate the accuracy and robustness in the MIBPB prediction of electrostatic solvation free energies (ΔG_{el}). Table S1, in the Supporting Information, reports the values ΔG_{el} for all

Table 1. R^2 values and best fitting lines of electrostatic solvation free energies with different grid sizes.

	Grid sizes (pair)	R^2	Best fitting line
DNA-drug	(0.2,0.3)	1.0000	$y=1.0000x-0.0196$
	(0.2,0.4)	1.0000	$y=1.0000x-0.0081$
	(0.2,0.5)	1.0000	$y=1.0001x-0.0621$
	(0.2,0.6)	1.0000	$y=1.0001x-0.2230$
	(0.2,0.7)	1.0000	$y=1.0003x-0.2537$
	(0.2,0.8)	1.0000	$y=1.0003x-0.4161$
	(0.2,0.9)	1.0000	$y=1.0003x-0.2999$
	(0.2,1.0)	1.0000	$y=1.0005x-0.0066$
	(0.2,1.1)	1.0000	$y=1.0004x-0.2485$
Barnase-barstar	(0.2,0.3)	1.0000	$y=1.0002x+0.1590$
	(0.2,0.4)	1.0000	$y=1.0005x+0.3524$
	(0.2,0.5)	1.0000	$y=1.0012x+0.8735$
	(0.2,0.6)	1.0000	$y=1.0010x-0.2246$
	(0.2,0.7)	1.0000	$y=1.0017x-0.3748$
	(0.2,0.8)	1.0000	$y=1.0009x-0.9576$
	(0.2,0.9)	0.9999	$y=1.0015x+0.4749$
	(0.2,1.0)	0.9999	$y=0.9986x-2.9739$
	(0.2,1.1)	0.9997	$y=0.9972x-4.3801$
RNA-peptide	(0.2,0.3)	1.0000	$y=1.0000x-0.0445$
	(0.2,0.4)	1.0000	$y=1.0000x-0.1333$
	(0.2,0.5)	1.0000	$y=1.0000x-0.3343$
	(0.2,0.6)	1.0000	$y=1.0000x-0.1916$
	(0.2,0.7)	1.0000	$y=1.0001x-0.5377$
	(0.2,0.8)	1.0000	$y=1.0001x-0.8198$
	(0.2,0.9)	1.0000	$y=1.0002x-0.9564$
	(0.2,1.0)	1.0000	$y=1.0003x-0.8868$
	(0.2,1.1)	1.0000	$y=1.0005x-2.2504$

the 51 complexes and associated 102 components studied in this work. Finally, we examine the performance of our solver by considering the relative absolute error, the difference between results obtained with coarser and the finest grid spacings, defined as follows

$$\text{Relative absolute error} \doteq \left| \frac{\Delta G_{\text{el},h} - \Delta G_{\text{el},h=0.2}}{\Delta G_{\text{el},h=0.2}} \right|. \quad (10)$$

Figure 3 illustrates the averaged relative absolute errors, that is, the average of relative absolute errors designated in eq. (10) over all the 153 discussed molecules, at different mesh sizes. It can be seen from Figure 3 that the averaged relative absolute errors at all studied cases are less than 0.31%, and for any grid spacing smaller than 1.1 Å, these errors are always below 0.2%. This behavior further indicates the grid size independence of our PB solver over the normal grid-size range in molecular biophysical applications.

The influence of grid spacing in $\Delta\Delta G_{\text{el}}$ estimation

Motivated by well-converged estimations of electrostatic solvation free energies at very coarse grid spacings as previously discussed, we are interested in predicting the binding free energies for all RNA-drug, barnase-barstar, and RNA-peptide complexes using our MIBPB package.

Similar to the study of the convergence of ΔG_{el}, we correlate the binding free energy calculated at the finest grid spacing, $h=0.2$ Å, and ones estimated at coarser mesh sizes, $h=0.3$ Å,···, 1.1 Å. Figure 4 illustrates these relationships with the

regression lines whose parameters are revealed in Table 2. As the previous discussion confirms MIBPB solver can produce very good R-squared values even at very coarse grid spacings, it is interesting to explore whether a similar behavior can be found for binding energy estimation. Indeed, the PB binding energy estimation behaves the same as the PB solvation calculation in our MIBPB technique. Specifically, R^2 is always 1 at the fine mesh, $h=0.3$ Å. Moreover, these values are still satisfactory at relatively coarser mesh sizes. For example, at the grid spacing of $h = 1.1$ Å, the R^2 and slope of the regression line for DNA-drug, barnase-barstar, and RNA-peptide complexes are, respectively, (0.9747, 1.0081), (0.8002, 0.8187), and (0.9998, 0.9937). Our statistical measures strongly support the reliable binding energy prediction of our solver at coarse grid sizes. Supporting Information Table S4 displays the binding free energy for all complexes with different grid spacings. As can be seen from Supporting Information Table S4, the difference between binding energies at coarse meshes and the finest mesh, $h=0.2$ Å, is mostly less than 10 kcal/mol for all complexes.

The trend of binding free energy at different grid spacings can be seen clearly in Figure 5 which plots $\Delta\Delta G_{\text{el}}$ against grid sizes varying between 0.2 and 1.1 Å for DNA-drug complexes. Similar figures for barnase-barstar and RNA-peptide complexes can be referred to Figs. S1 and S2 in the Supporting Information. Based on these figures, our solver can rank the binding free energy for DNA-drug complexes at grid spacing of 0.6 Å, barnase-barstar complexes at grid spacing of 0.6 Å, and RNA-peptide complexes at significantly coarse grid spacing of 1.1 Å. To further assess the reliable estimates of binding energy of our MIBPB solver, we consider the absolute difference between results computed at a coarser grid spacing and the finest grid spacing defined by

$$\delta\Delta\Delta G_{\text{el}} = |\Delta\Delta G_{\text{el},h} - \Delta\Delta G_{\text{el},h=0.2}|. \quad (11)$$

Figure 6 plots the averaged absolute errors, $\overline{\delta\Delta\Delta G_{\text{el}}}$, that is, the average of absolute errors defined in eq. (11) over all 51 complexes, at different mesh sizes. It is seen that even the use
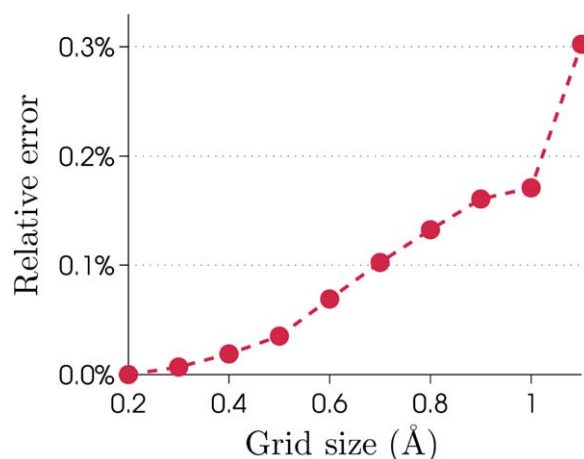

Figure 3. Averaged relative absolute error of the electrostatic solvation free energies for all the 153 molecules with mesh size refinements from 1.1 to 0.2 Å. [Color figure can be viewed at wileyonlinelibrary.com]
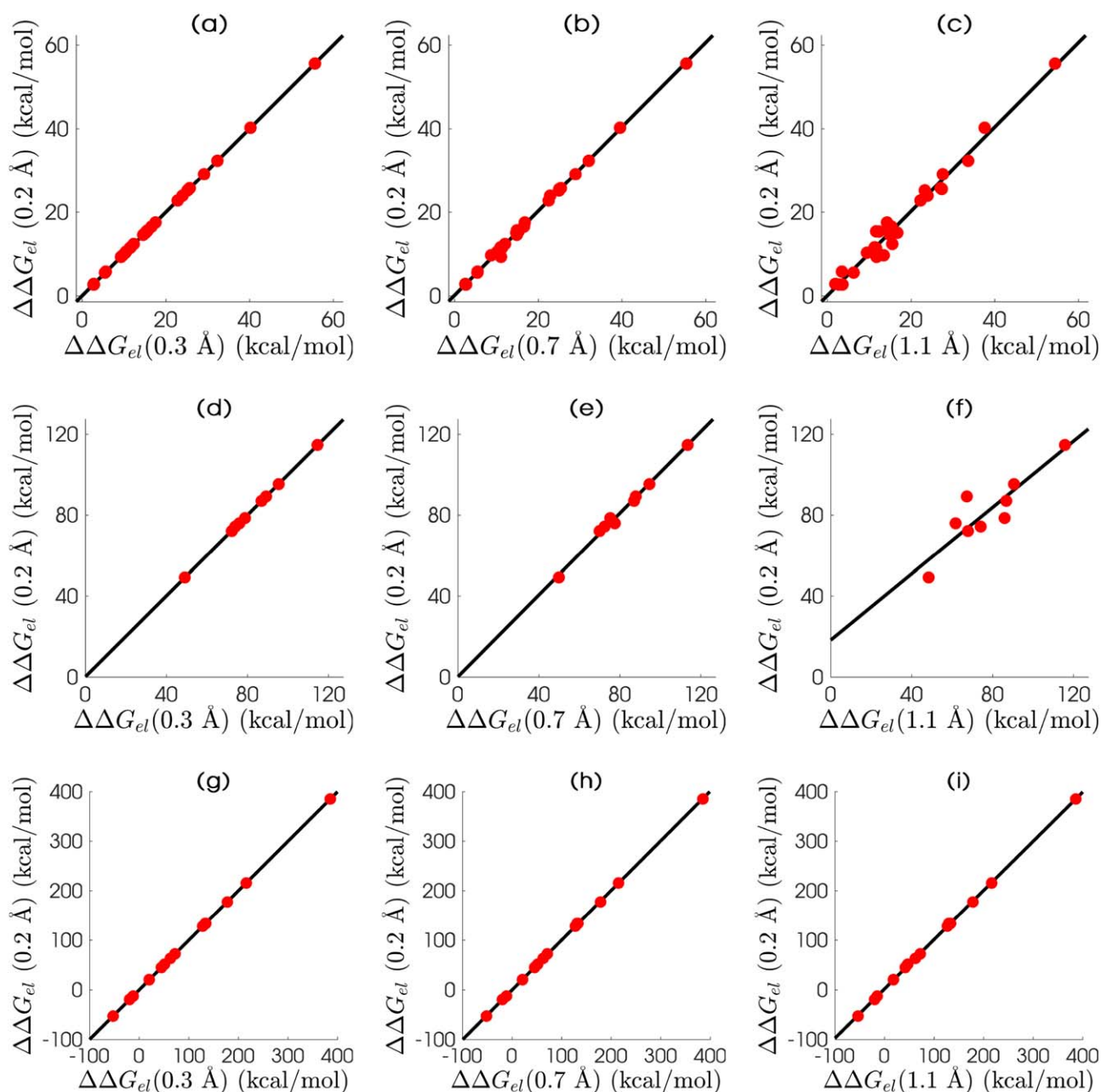
Figure 4. Electrostatic binding free energy, for all complexes with different grid sizes plotted against the one computed with a finest grid size of $h=0.2$ Å. a) DNA-drug with pair (0.2 Å, 0.3 Å); b) DNA-drug with pair (0.2 Å, 0.7 Å); c) DNA-drug with pair (0.2 Å, 1.1 Å); d) Barnase-barstar with pair (0.2 Å, 0.3 Å); e) Barnase-barstar with pair (0.2 Å, 0.7 Å); f) Barnase-barstar with pair (0.2 Å, 1.1 Å); g) RNA-peptide with pair (0.2 Å, 0.3 Å); h) RNA-peptide with pair (0.2 Å, 0.7 Å); i) RNA-peptide with pair (0.2 Å, 1.1 Å). [Color figure can be viewed at wileyonlinelibrary.com]

of grid spacing of 0.7 Å still delivers an averaged binding calculation error under 1 kcal/mol for this set of complexes. Therefore, we can draw a conclusion that the common use of grid size being 0.5 Å is still adequate for predicting the binding energy free without producing a misleading result.

Grid positioning error is another feature to validate the robustness and accuracy of a PB solver. To examine such numerical error for our MIBPB solver, we consider two protein complexes with PDBIDs: 360d and 1hji. To estimate the standard deviation, σ_{bd} in $\Delta\Delta G_{el}$, we randomly generate 29 grid positions around the initial origin with the amplitude of the random seed being $\pm 0.5h$, where $h=0.5$ Å is the grid

spacing. Then $\Delta\Delta G_{el}$ is evaluated at all of the 30 grid positions. Figure 7 plots electrostatic binding energies at 30 distinct samples of grid positions, including the original one marked by Sample 0 on the graph. The σ_{bd} values of complexes 360d and 1hji are found to be 0.18 and 0.21, respectively. These results indicate that the MIBPB solver is not sensitive to grid position.

To further support our calculations, we have used PBSA, Delphi, and APBS for electrostatic energy calculations at the grid size of 0.2 Å. We note that results obtained from these solvers are in excellent agreements, that is, $R^2 > 0.98$, with ours. The electrostatic energies calculated by PBSA, Delphi, and APBS solvers are listed in Table S2 of Supporting Information.

Table 2. R^2 values and best fitting lines of electrostatic binding free energies with different grid sizes.

	Grid sizes (pair)	R^2	Best fitting line
DNA-drug	(0.2,0.3)	1.0000	$y = 0.9993x + 0.0194$
	(0.2,0.4)	0.9999	$y = 0.9987x + 0.0273$
	(0.2,0.5)	0.9998	$y = 1.0028x + 0.0164$
	(0.2,0.6)	0.9991	$y = 1.0047x + 0.2256$
	(0.2,0.7)	0.9982	$y = 1.0074x + 0.1394$
	(0.2,0.8)	0.9966	$y = 1.0110x + 0.1484$
	(0.2,0.9)	0.9906	$y = 0.9655x + 1.2385$
	(0.2,1.0)	0.9875	$y = 0.9827x + 0.5894$
	(0.2,1.1)	0.9747	$y = 1.0081x + 0.0709$
Barnase-barstar	(0.2,0.3)	0.9999	$y = 0.9974x + 0.2035$
	(0.2,0.4)	0.9995	$y = 0.9997x - 0.0492$
	(0.2,0.5)	0.9923	$y = 1.0318x - 2.7755$
	(0.2,0.6)	0.9946	$y = 0.9878x + 1.5525$
	(0.2,0.7)	0.9932	$y = 1.0090x + 0.1819$
	(0.2,0.8)	0.9883	$y = 0.9766x + 3.7333$
	(0.2,0.9)	0.9493	$y = 0.9382x + 5.3970$
	(0.2,1.0)	0.9384	$y = 1.0912x - 3.8377$
	(0.2,1.1)	0.8002	$y = 0.8187x + 18.2837$
RNA-peptide	(0.2,0.3)	1.0000	$y = 0.9997x - 0.0655$
	(0.2,0.4)	1.0000	$y = 1.0001x - 0.1106$
	(0.2,0.5)	1.0000	$y = 1.0012x - 0.2755$
	(0.2,0.6)	1.0000	$y = 0.9999x + 0.2021$
	(0.2,0.7)	0.9999	$y = 1.0037x - 0.3756$
	(0.2,0.8)	1.0000	$y = 1.0004x + 0.6673$
	(0.2,0.9)	0.9999	$y = 0.9927x + 1.9755$
	(0.2,1.0)	0.9997	$y = 0.9923x + 2.8775$
	(0.2,1.1)	0.9998	$y = 0.9937x + 1.7992$

Concluding Remarks

PB theory is an established model for biomolecular electrostatic analysis and has been widely used in electrostatic solvation
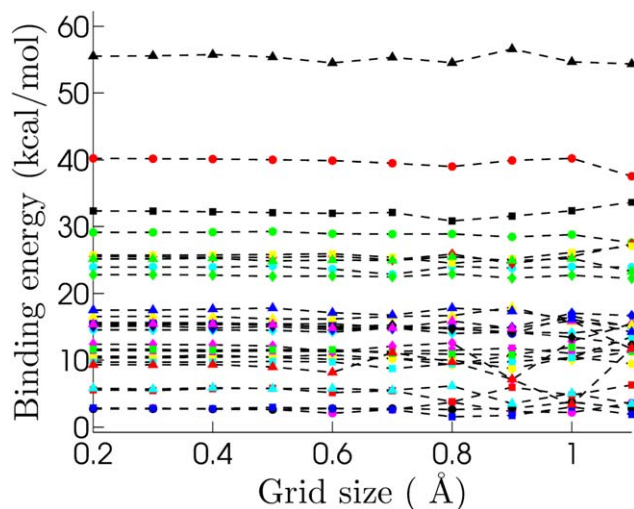

Figure 5. Binding electrostatic energy for DNA-drug complexes with grid sizes from 0.2 to 1.1 Å. The markers and PDBIDs are as follows yellow circle: 102d, magenta circle: 109d, cyan circle: 121d, green circle: 127d, red circle: 129d, blue circle: 166d, black circle: 195d, yellow diamond: 1d30, magenta diamond: 1d63, cyan diamond: 1d64, green diamond: 1d86, red diamond: 1dne, blue diamond: 1eel, black diamond: 1fmq, yellow square: 1fms, magenta square: 1jtl, cyan square: 1lex, green square: 1prp, red square: 227d, blue square: 261d, black square: 264d, yellow triangle: 289d, magenta triangle: 298d, cyan triangle: 2dbe, green triangle: 302d, red triangle: 311d, blue triangle: 328d, black triangle: 360d. [Color figure can be viewed at wileyonlinelibrary.com]
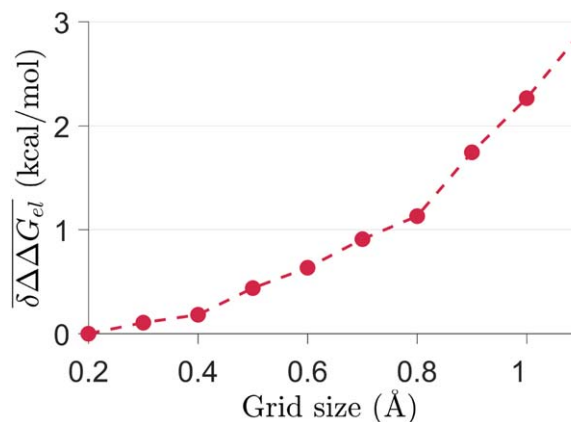

Figure 6. Averaged absolute error of the binding free energies for all the 51 complexes with mesh size refinements from 1.1 to 0.2 Å. [Color figure can be viewed at wileyonlinelibrary.com]

ΔG_{el} and binding energy $\Delta\Delta G_{el}$ estimations. Accurate, efficient, and reliable calculation of solvation and binding free energies is of crucial importance to physics, chemistry, biology, and material science. In this work, we use the MIBPB software[18,28] to estimate electrostatic solvation free energy, ΔG_{el}, and binding free electrostatic energy, $\Delta\Delta G_{el}$, for the three sets of biomolecular complexes, namely, DNA-drug complexes, barnase-barstar complexes, and RNA-peptide complexes. The popular SES is adopted in the present work. In our ΔG_{el} estimation, the averaged relative absolute error computed at a relatively coarse grid size of 1.1 Å against the finest grid size of 0.2 Å over 153 studied biomolecules is less than 0.31%. The same error obtained at the grid size of 1.0 Å is less than 0.2%. These results indicate the reliability of using the MIBPB solver at the grid spacing of 1.0 Å or even 1.1 Å for electrostatic solvation analysis. The robustness and accuracy of MIBPB solver for estimates of ΔG_{el} have been reported for 24 proteins in the literature.[18,28] This characteristics has been confirmed again in the present work for DNA-drug complexes, barnase-barstar complexes, and RNA-peptide complexes.

The well-converged ΔG_{el} produced by our solver enables a promising performance in predicting $\Delta\Delta G_{el}$ at a coarse grid
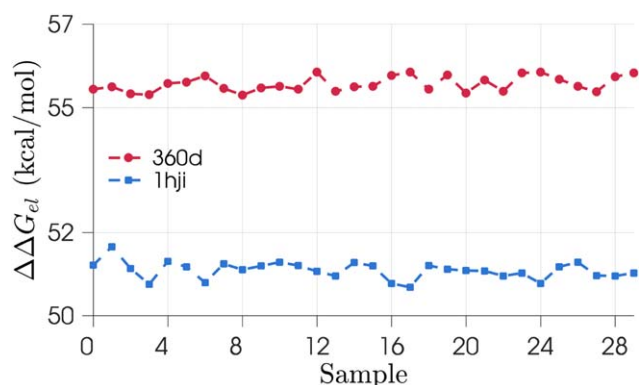

Figure 7. Binding energies of two complexes PDB IDs: 360d (marked by circle) and 1hji (marked by square) at 30 different grid positions. [Color figure can be viewed at wileyonlinelibrary.com]

Journal of COMPUTATIONAL CHEMISTRY

spacing. Indeed, numerical estimates of $\Delta\Delta G_{el}$ in the current work reveals that $\Delta\Delta G_{el}$ obtained at a 1.1 Å grid spacing mostly differ by less than 10 kcal/mol from that achieved using a 0.2 Å grid spacing. Moreover, MIBPB solver conducted at grid size of 0.6 Å perfectly produces a well-converged $\Delta\Delta G_{el}$, and qualitatively ranks the complexes in term of their binding free energies. Therefore, the current results support an opinion that the widely used grid size of 0.5 Å can give reliable and accurate enough predictions of both electrostatic free energy[34] and binding free energy.

To develop highly accurate, robust, and reliable PB solvers for biomolecular electrostatics, it is crucial to validate one's numerical methods by appropriate norms and against realistic problems. We emphasize that as an elliptic interface problem, it is important to measure the convergence of PB solvers in the L_∞ norm, or maximum absolute error, because integral norms, such as L_1 and L_2, are insensitive to the performance of numerical methods near the interface. Additionally, the convergence should be tested by solving the PB equation, rather than by calculating the solvation free energy. Finally, validation should be carried out using the SESs of proteins, rather than regular and simple surfaces, such as a sphere.

For protein-protein interactions involving multiprotein complexes, a multiscale approach can be used to divide the computational domain into small overlapping subdomains.[35] On each subdomain, a finer grid is used. Iterations between the global mesh and subdomain meshes are required to achieve a uniform convergence. A multiscale MIBPB technique is under our consideration.

Acknowledgment

[1] M. K. Gilson, K. Sharp, B. Honig, *J. Comput. Chem.* **1987**, 9, 327.
[2] M. K. Gilson, M. E. Davis, B. A. Luty, J. A. McCammon, *J. Phys. Chem.* **1993**, 97, 3591.
[3] K. Talley, C. Ng, M. Shoppell, P. Kundrotas, E. Alexov, *PMC Biophys.* **2008**, 1, 1.
[4] Y. C. Zhou, M. Feig, G. W. Wei, *J. Comput. Chem.* **2008**, 29, 87.
[5] P. Ren, J. Chun, D. G. Thomas, M. J. Schnieders, M. Marucho, J. Zhang, N. A. Baker, *Q. Rev. Biophys.* **2012**, 45, 427.
[6] S. Jo, M. Vargyas, J. Vasko-Szedlar, B. Roux, W. Im, *Nucleic Acids Res.* **2008**, 36, W270.
[7] N. A. Baker, D. Sept, M. J. Holst, J. A. Mccammon, *IBM J. Res. Dev.* **2001**, 45, 427.
[8] J. Ying, D. Xie, *J. Comput. Phys.* **2015**, 298, 636.
[9] W. H. Geng, R. Krasny, *J. Comput. Phys.* **2013**, 247, 62.
[10] B. Lu, X. Cheng, J. Huang, J. A. McCammon, *Comput. Phys. Commun.* **2013**, 184, 2618.
[11] J. Wang, C. H. Tan, Y. H. Tan, Q. Lu, R. Luo, *Commun. Comput. Phys.* **2008**, 3, 1010.
[12] Q. Cai, M. J. Hsieh, J. Wang, R. Luo, *J. Chem. Theory Comput.* **2009**, 6, 203.
[13] L. Li, C. Li, S. Sarkar, J. Zhang, S. Witham, Z. Zhang, L. Wang, N. Smith, M. Petukh, E. Alexov, *BMC Biophys.* **2012**, 5, 9.
[14] W. Rocchia, S. Sridharan, A. Nicholls, E. Alexov, A. Chiabrera, B. Honig, *J. Comput. Chem.* **2002**, 23, 128.
[15] N. A. Baker, D. Sept, S. Joseph, M. J. Holst, J. A. McCammon, *Proc. Natl. Acad. Sci. USA* **2001**, 98, 10037.
[16] C. Wang, J. Wang, Q. Cai, Z. Li, H. K. Zhao, R. Luo, *Comput. Theor. Chem.* **2014**, 1, 34.
[17] M. Mirzadeh, M. Theillard, F. Gibou, *J. Comput. Phys.* **2011**, 230, 2125.
[18] D. Chen, Z. Chen, C. Chen, W. H. Geng, G. W. Wei, *J. Comput. Chem.* **2011**, 32, 657.
[19] F. M. Richards, *Annu. Rev. Biophys. Bioeng.* **1977**, 6, 151.
[20] M. L. Connolly, *J. Appl. Crystallogr.* **1983**, 16, 548.
[21] M. F. Sanner, A. J. Olson, J. C. Spehner, *Biopolymers* **1996**, 38, 305.
[22] Y. C. Zhou, G. W. Wei, *J. Comput. Phys.* **2006**, 219, 228.
[23] Y. C. Zhou, S. Zhao, M. Feig, G. W. Wei, *J. Comput. Phys.* **2006**, 213, 1.
[24] S. N. Yu, W. H. Geng, G. W. Wei, *J. Chem. Phys.* **2007**, 126, 244108.
[25] S. N. Yu, Y. C. Zhou, G. W. Wei, *J. Comput. Phys.* **2007**, 224, 729.
[26] S. N. Yu, G. W. Wei, *J. Comput. Phys.* **2007**, 227, 602.
[27] K. L. Xia, M. Zhan, G. W. Wei, *J. Comput. Appl. Math.* **2014**, 272, 195.
[28] W. Geng, S. Yu, G. W. Wei, *J. Chem. Phys.* **2007**, 127, 114106.
[29] S. Decherchi, W. Rocchia, *PLoS One* **2013**, 8, e59744.
[30] B. Liu, B. Wang, R. Zhao, Y. Tong, G. W. Wei, *J. Comput. Chem.* **2017**, 38, 446.
[31] E. F. Pettersen, T. D. Goddard, C. C. Huang, G. S. Couch, D. M. Greenblatt, E. C. Meng, T. E. Ferrin, *J. Comput. Chem.* **2004**, 25, 1605.
[32] M. Feig, A. Onufriev, M. S. Lee, W. Im, D. A. Case, C. L. Brooks, *J. Comput. Chem.* **2004**, 25, 265.
[33] C. M. Reyes, P. A. Kollman, *J. Mol. Biol.* **2000**, 297, 1145.
[34] D. Shivakumar, J. Williams, Y. Wu, W. Damm, J. Shelley, W. Sherman, *J. Chem. Theory Comput.* **2010**, 6, 1509.
[35] L. Li, J. Alper, E. Alexov, *Sci. Rep.* **2016**, 6, 23249.

ChemistryViews